

Effect of Aligned Magnetic Field and Thermal Radiation of a Casson Fluid Over a Stretching Sheet in a Thermally Stratified Medium

Chenna Sumalatha^{1,*}, Bandari Shankar², and T. Srinivasulu³

¹Research Scholar in Department of Mathematics, Osmania University, Hyderabad 500001, India

²Department of Mathematics, Osmania University, Hyderabad 500001, India

³Department of Mathematics, Mahabubnagar Vidya Samithi Govt. Degree College, Mahabubnagar 509001, Telangana, India

The investigation has been carried out to analyze the effect of Aligned magnetic field and Thermal radiation of a Casson fluid over a stretching sheet in a Thermally stratified medium. The governing differential equations of the problem are transformed into a set of nonlinear coupled ordinary differential equations using similarity transformations. The resulting equations are solved numerically by using an implicit finite difference method known as Keller Box method. Results are shown graphically in the velocity profile and the temperature profile with different values of physical parameters like suction parameter, magnetic parameter, Aligned magnetic parameter, Prandtl number, Casson parameter, Radiation parameter, Stratification parameter, A comparison with previously published work has been carried out and the results are found to be in good agreement. We noticed that the velocity profile decreases with an increase in the Casson fluid parameter and Suction parameter. The temperature profile decreases with an increase in stratification parameter where as temperature gradient increases.

Copyright: American Scientific Publishers
 Delivered by Ingenta

KEYWORDS: MHD, Aligned Magnetic Field, Casson Fluid, Radiation, Suction, Stretching Sheet, Thermally Stratified Medium.

1. INTRODUCTION

MHD is the study of the flow of electrically conducting fluids in a magnetic field. In fluid mechanics, the study of MHD flow over a stretching sheet has wide applications in industrial problems, such as glass manufacturing, nuclear reactors, geophysics, induction of flow meter, plasma studies, paper production, and purification of crude oil. Pavlov¹ explained the effect of external magnetic field on the MHD flow over a stretching sheet. MHD stagnation point flow of Casson fluid and heat transfer over a stretching sheet with thermal radiation was examined by Krishnendu Bhattacharya.² Ibrahim³ studied the boundary layer flow and heat transfer of a Nanofluid over a permeable stretching sheet with the effects of MHD, thermal radiation and slip boundary conditions. Vijayalaxmi⁴ studied the effect of aligned magnetic field on the slip flow of Casson Nanofluid over a nonlinear stretching sheet with chemical reaction. The flow of Nanofluid over an

exponential stretching sheet in porous media with the effects of the Aligned magnetic field and cross diffusion had been investigated by Sulochana.⁵ The excellent concerning articles on this topic can be found in Refs. [6–8].

The effect of stratification plays an important role in heat transfer analysis. It is essentially the formation or deposition of layers. This phenomenon may arise due to a continuous discharge of the thermal boundary layer in the medium, such as, a heated vertical surface embedded in a porous bed which is of limited extent in the direction of the plate. Swati Mukhopadhyay⁹ analyzed the MHD boundary layer flow and heat transfer towards an exponentially stretching sheet embedded in a thermally stratified medium subject to suction. Thermally stratified stagnation point flow of Casson fluid with slip conditions was examined by Tasawar Hayat.¹⁰ Thermal and solutal stratification on heat and mass transfer induced due to a nanofluid over a porous vertical plate investigated by Kandasamy.¹¹ The problem of stratified medium on a stretching sheet for different cases of fluid has been studied by different researchers.^{12–14}

The Casson fluid model is one of the Non-Newtonian fluid model which has high viscosity and not obey the

*Author to whom correspondence should be addressed.
 Email: Sumalatha.chenna@gmail.com
 Received: 4 November 2017
 Accepted: 11 December 2017

Newton's law of viscosity. This fluid was first introduced by Casson (1995). Kalaivanan¹⁵ studied the effect Aligned magnetic field on the slip flow of Casson fluid over a stretching sheet. MHD Stagnation Point Flow of a Casson Nanofluid towards a Radially Stretching Disk with Convective Boundary Condition in the Presence of Heat Source/Sink was examined by Prabhakar.¹⁶ Some studies include Casson fluid can be found in Refs. [17, 18].

Nowadays the researchers are very interested to study the flow caused by steady or unsteady stretching sheets. A broad effort had been made to gain information regarding the stretching flow problems in various situations. The exact solution for the flow due to stretching of flat surface was first obtained by Crane.¹⁹ Subhash able²⁰ studied a mathematical analysis MHD flow of a Heat transfer in a liquid film over an unsteady stretching surface with viscous dissipation in presence of external magnetic field. Viscous Dissipation and Radiation Effects on MHD Boundary Layer Flow of a Nanofluid Past a Rotating Stretching Sheet was proposed by Wahiduzzaman.²¹ Heat and mass transfer on a stretching sheet with suction or blowing was studied by Gupta and Gupta.²² MHD flow and heat transfer over a stretching sheet with variable fluid viscosity has been examined by Mukhopadhyay.²³ Khan and Pop²⁴ discussed the Boundary layer flow of a Nanofluid past a stretching sheet.

Thermal Radiation and slip effects on MHD stagnation point Flow of non-Newtonian over a convective Stretching surface was analysed by Prabhakar.²⁵ Bidin and Nazar²⁶ explained the effect of thermal radiation on the steady laminar two-dimensional boundary layer flow and heat transfer over an exponentially stretching sheet. Dharmender Reddy²⁷ examined the effect of Thermal radiation and viscous dissipation on MHD boundary layer flow and heat transfer over a porous exponentially stretching sheet. Ganeswara Reddy²⁸ examined the Thermal Radiation Effects on MHD Stagnation Point Flow of Nanofluid Over a Stretching Sheet in a Porous Medium. The Keller-Box method introduced by Keller²⁹ is one of the best numerical methods basically it's a mixed finite volume method which consists in taking the average of a conservation law and of the associated constitutive law at the level of the same mesh cell. Sarif³⁰ worked the numerical solution of the steady boundary layer flow and heat transfer over a stretching sheet with Newtonian heating by using a Keller box method.

Motivated by the above articles, the aim of the present paper is to study the effects of Aligned magnetic field and Thermal radiation of a Casson fluid over a stretching sheet in a Thermally stratified medium in the presence of suction parameter. The basic governing equations are converted into ordinary differential equations by applying suitable similarity transformations and those equations were solved numerically by using finite difference method called as the Keller Box method.

2. MATHEMATICAL FORMULATION

A steady incompressible two-dimensional laminar free convective electrically conducting viscous fluid flow along stretches sheet embedded in a thermally stratified medium in the presence of aligned magnetic field is considered for theoretical study. The x -axis is taken along the stretching sheet and y is the coordinate normal to the surface. Along with these the fluid is permitted by an aligned magnetic field. The fluid is electrically conducting under the influence of magnetic field B_0 normal to the stretching sheet. The induced magnetic field is assumed to be small compared to the applied magnetic field. So it is neglected. Assume that the sheet of temperature is $T_W(x)$ and is embedded in a thermally stratified medium of variable ambient temperature $T_\infty(x)$ where $T_W(x) > T_\infty(x)$ it is assumed that $T_W(x) = T_0 + bx$, $T_\infty(x) = T_0 + cx$ where T_0 is the reference temperature, $b > 0$, $c \geq 0$ are constants. All the fluid properties are assumed to be constant.

The rheological equation of state for an isotropic and incompressible flow of the Casson fluid is given by

$$\tau_{ij} = 2(\mu_B + p_y/\sqrt{2\pi})e_{ij}, \quad \pi > \pi_c,$$

$$2(\mu_B + p_y/\sqrt{2\pi_c})e_{ij}, \quad \pi < \pi_c$$

Where μ_B and p_y the plastic dynamic viscosity, yield stress of the fluid respectively. Similarly π is the product of the component of deformation rate by itself, $\pi = e_{ij}e_{ij}$, e_{ij} is the (i, j) -th component of the deformation rate and π_c is a critical value of this product based on the non-Newtonian model.

Under the above assumptions, the governing equations for the above flow are given by the following equations.

The continuity equation

$$\frac{\partial u}{\partial x} + \frac{\partial v}{\partial y} = 0 \quad (1)$$

The momentum equation

$$u \frac{\partial u}{\partial x} + v \frac{\partial u}{\partial y} = \vartheta \left(1 + \frac{1}{\beta} \right) \frac{\partial^2 u}{\partial y^2} - \frac{\sigma B_0^2}{\rho} \sin^2(\gamma) u = 0 \quad (2)$$

The energy equation

$$u \frac{\partial T}{\partial x} + v \frac{\partial T}{\partial y} = \alpha \frac{\partial^2 T}{\partial y^2} - \frac{1}{\rho C_p} \frac{\partial q_r}{\partial y} \quad (3)$$

Using the Roseland approximation $q_r = -(4\sigma^*/3k^*) \partial T^4 / \partial y$ is obtained where σ^* is the Stefan-Boltzmann constant and k^* is the absorption coefficient. We presume that the temperature variation within the flow is such that T^4 may be expanded in a Taylor's series. Expanding T^4 about T_∞ and neglecting higher-order terms we get $T^4 = 4T_\infty^3 T - 3T_\infty^4$, then q_r becomes

$$q_r = -\frac{16T_\infty^3 \sigma^*}{3k^*} \frac{\partial T}{\partial y}$$

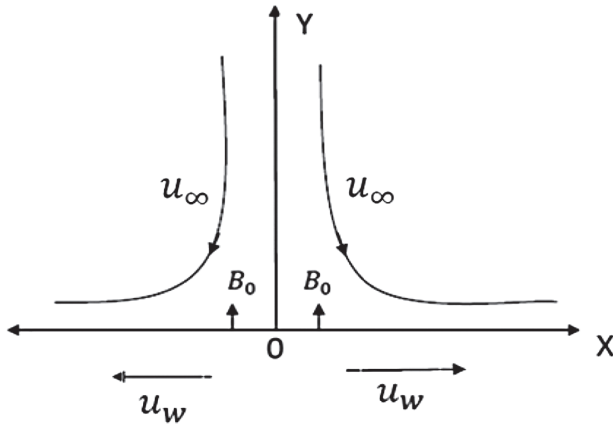


Fig. 1. Physical model and coordinate system.

Substitute \$q_r\$ value in (3) we obtain

$$u \frac{\partial T}{\partial x} + v \frac{\partial T}{\partial y} = \alpha \frac{\partial^2 T}{\partial y^2} + \frac{16T_\infty^3 \sigma^*}{3k^* \rho C_p} \frac{\partial^2 T}{\partial y^2} \tag{4}$$

Where \$u, v\$ are the components of velocity in \$x, y\$ directions respectively, \$\nu = \mu/\rho\$ is the kinematic viscosity, \$\mu\$ is the coefficient of fluid viscosity, \$\rho\$ is the fluid density, \$\beta = \mu_B \sqrt{2\pi_c/p_y}\$ is the Casson fluid parameter and \$\kappa\$ is the thermal conductivity, \$C_p\$ is the specific heat at constant pressure.

The suitable boundary conditions are given by

$$\begin{aligned} u = U_w(x) = U_0x, \quad v = -V(x) = V_0x \\ T = T_w(x) \quad \text{at } y \rightarrow 0 \\ u \rightarrow 0, \quad T = T_\infty(x) \quad \text{at } y \rightarrow \infty \end{aligned} \tag{5}$$

Here \$U_w(x) = U_0x\$ is the stretching velocity, \$U_0\$ is the reference velocity, \$V(x) > 0\$ is velocity of suction and \$V(x) < 0\$ is velocity of blowing, \$V(x) = V_0x\$, a special type of velocity at the wall is considered. \$V_0\$ is the initial strength of suction.

The stream function \$\psi(x, y)\$ is defined by \$u = \partial\psi/\partial y\$ and \$v = -\partial\psi/\partial x\$, such that the continuity Eq. (1) is satisfied automatically. With the help of following similarity transformations, the non linear partial differential Equations (2) and (4) were transformed into coupled non linear ordinary differential equations.

$$\begin{aligned} \eta = y\sqrt{\frac{U_0}{\nu}}x, \quad \psi = \sqrt{U_0\nu}xf(\eta), \\ u = U_0xf'(\eta), \quad \theta(\eta) = \frac{T - T_\infty}{T_w - T_\infty} \end{aligned} \tag{6}$$

The Eqs. (1), (2) and (4) are transformed in to coupled non linear ordinary differential equations as follows.

$$\left(1 + \frac{1}{\beta}\right) f''' + ff'' - f'^2 - Mf' \sin^2(\gamma) = 0 \tag{7}$$

$$\left(1 + \frac{4}{3}R_d\right) \theta'' + Pr(f\theta' + f'\theta - Stf') = 0 \tag{8}$$

The associated boundary conditions becomes

$$\begin{aligned} f'(\eta) = 1, \quad f(\eta) = S, \quad \theta(\eta) = 1 - St \quad \text{at } \eta \rightarrow 0 \\ f'(\eta) \rightarrow 0, \quad \theta(\eta) \rightarrow 0 \quad \text{at } \eta \rightarrow \infty \end{aligned} \tag{9}$$

Where the prime denotes differentiation with respect to \$\eta\$. \$M = \sigma B_0^2/(\rho U_0)\$ is the magnetic parameter, \$\gamma\$ is the aligned angle, \$\beta\$ is Casson parameter, \$Pr = \nu/\alpha\$ is the Prandtl number, \$S = V_0/\sqrt{U_0\nu} > 0\$ (or \$< 0\$) is the suction (or blowing), \$St = c/b\$ is the stratification parameter. \$St > 0\$ implies a stably stratified environment, while \$St = 0\$ represents an unstratified environment. \$R_d = 4\sigma^*T_\infty^3/(kk^*)\$ is the radiation parameter.

Hence the dimensionless form of Skin friction \$C_f\$ and the Local Nusselt number \$Nu_x\$ are given by

$$C_f(Re_x)^{1/2} = \left(1 + \frac{1}{\beta}\right) f''(0), \quad \frac{Nu_x}{(Re_x)^{1/2}} = -\theta'(0) \tag{10}$$

where \$Re_x = U_w x/\nu\$ is the local Reynolds number.

3. NUMERICAL PROCEDURE

The boundary value problem (7)–(8) together with the boundary conditions (9) are solved by a second order finite difference scheme known as the Keller Box method.²⁸ The numerical solutions are obtained in four steps as follows:

- Reduce the ordinary differential equations to a system of first order equations;
- write the difference equations for ordinary differential equations using central differences;
- linearize the algebraic equations by Newton’s method, and write them in matrix–vector form;
- solve the linear system by the block tri-diagonal elimination technique.

The step size \$\Delta\eta\$ and the position of the edge of the boundary layer \$\eta_\infty\$ are to be adjusted for different values of the parameters to maintain accuracy. For numerical calculations, a uniform step size of \$\Delta\eta = 0.01\$ is found to be satisfactory and the solutions are obtained with an error tolerance of \$10^{-6}\$ in all the cases. For brevity, the details of the solution procedure are not presented here.

4. RESULTS AND DISCUSSION

The non-linear ordinary differential equations Eqs. (7)–(8) with the boundary conditions (9) were solved numerically by the Keller Box method. The computation has been carried out for different values of governing parameters viz. Casson parameter \$\beta\$, suction parameter \$S\$, magnetic parameter \$M\$, Aligned magnetic parameter \$\gamma\$, Prandtl number \$Pr\$, Stratification parameter \$St\$, Radiation parameter \$R_d\$. The velocity, temperature profiles for different governing parameters have also been examined for both values of aligned magnetic parameter \$\gamma = 30^\circ\$ and \$\gamma = 90^\circ\$. The results obtained in the study are compared with the existing literature and found in good agreement which is presented in the Table I.

Table I. The comparison of the values of Nusselt number $-\theta'(0)$ for several values of Pr when $M = R_d = St = S = 0$ and $\beta = 10000, \gamma = 90^\circ$.

Pr	Bidin and Nazar ²⁶	Swati Mukhopadhyay ⁹	Present study
1	0.9547	0.9547	0.9547
2	1.4714	1.4714	1.4715
3	1.8961	1.8961	1.8961

Figure 2 shows that the velocity profile for the variation of the magnetic parameter M of both the values of Aligned magnetic parameter $\gamma = 30^\circ, 90^\circ$. It can be noticed that when magnetic parameter M increases the velocity profile decreases. This is because the increasing value of magnetic parameter M improves opposite force to the fluid flow direction called Lorentz force. This Lorentz force is a resistive force which opposes the motion of the fluid. This result gives rise in decreases in velocity of the fluid.

Figures 3(a)–(c) shows the influence of Suction parameter S for both the values of Aligned magnetic parameter $\gamma = 30^\circ, 90^\circ$ on velocity profile, temperature profile and shear stress respectively. From Figure 3(a) it is clear that the velocity profile is decreasing as increasing the values of suction parameter S . Due to increase of suction parameter S the amount of fluid particles were drawn into the wall, hence it decrease the boundary layer thickness. From Figure 3(b) we observe that the temperature decreases with increasing suction parameter. Here we are considered the wall suction is positive, this causes a decrease in thermal boundary layer thickness. Figure 3(c) shows that the shear stress decreases initially with increasing the suction parameter S , but finally shear stress increases significantly after a certain distance from the sheet.

The effect of the Radiation parameter R_d on the temperature profile has been depicted in Figure 4. From Figure 4

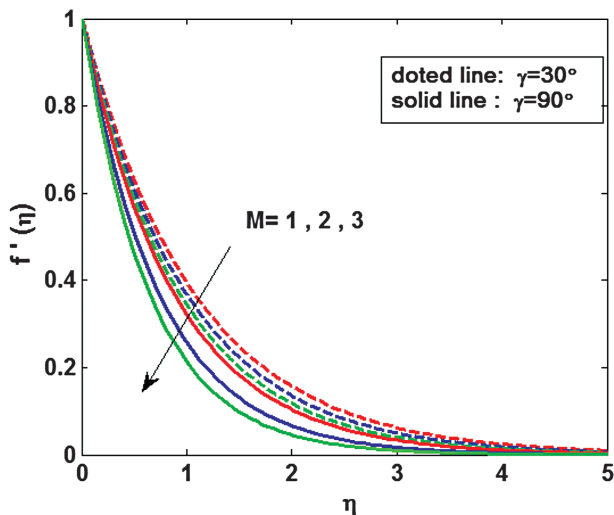


Fig. 2. Effect of magnetic parameter M on velocity profile where $Pr = 0.7, S = 1, \beta = 2, R_d = 0.5, St = 0.2$.

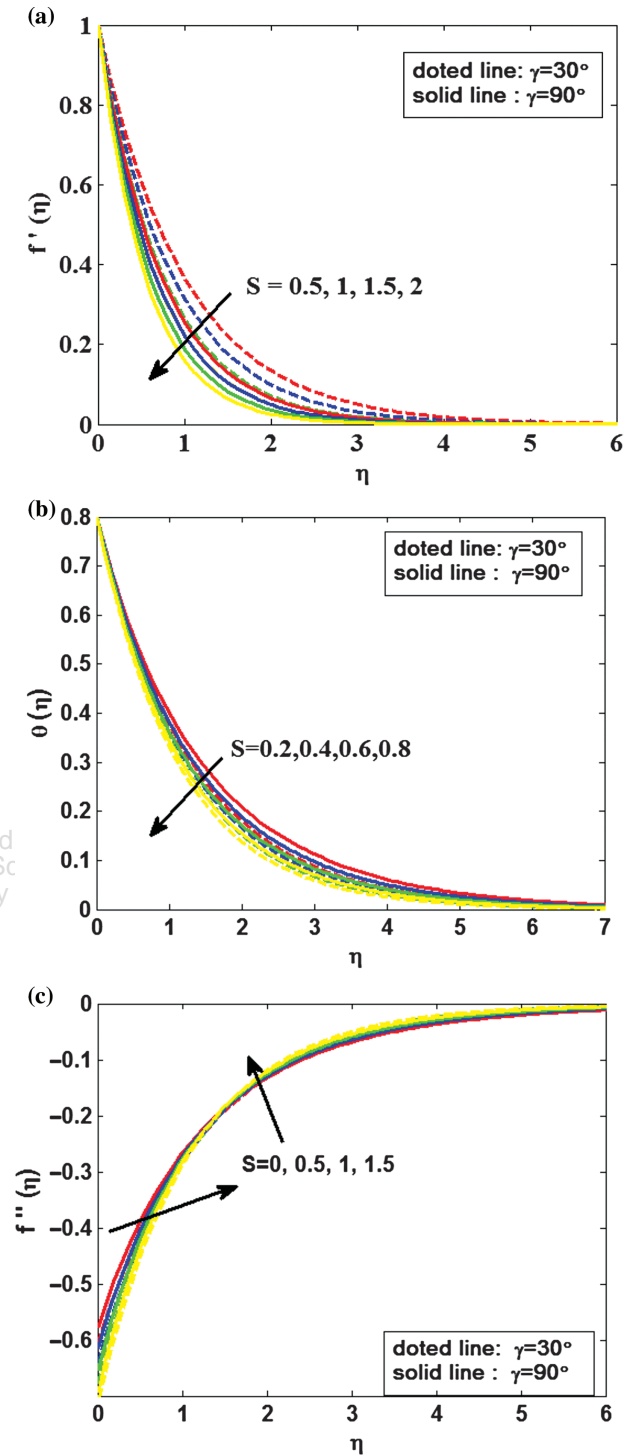


Fig. 3. (a) Effect of suction parameter S on velocity profile where $Pr = 0.7, M = 2, \beta = 2, R_d = 0.5, St = 0.2$. (b) Effect of suction parameter S on temperature profile where $Pr = 0.7, M = 2, \beta = 2, R_d = 0.5, St = 0.2$. (c) Effect of suction parameter S on shear stress $f''(\eta)$ where $Pr = 0.7, M = 2, \beta = 2, R_d = 0.5, St = 0.2$.

it is clear that the temperature and thermal boundary layer thickness is increasing with the increase of radiation parameter R_d . This is because the thermal radiation leads to heat transfer.

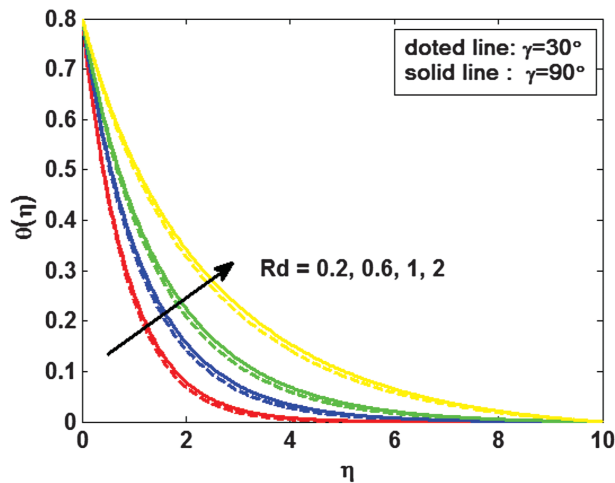


Fig. 4. Effect of thermal radiation parameter R_d on temperature profile where $Pr = 0.7$, $M = 2$, $\beta = 2$, $S = 1$, $St = 0.2$.

Figure 5 depicts the nature of the Prandtl number Pr on temperature profile. From the figure we noticed that an increase in Prandtl number Pr results in a decrease in the temperature distribution because the thermal boundary layer thickness decreases with an increase in Prandtl number Pr . An increase in Pr means the slow rate of thermal diffusion.

Figures 6(a) and (b) shows the influence of thermal stratification parameter St on temperature and temperature gradient respectively. From Figure 6(a) we noticed that the temperature decreases as the stratification parameter St increases. Obviously an increase in St means an increase in free-stream temperature. Therefore the thermal boundary layer thickness is decreases as an increase in stratification parameter St . The temperature gradient increases with an increase in stratification parameter St is depicted by Figure 6(b).

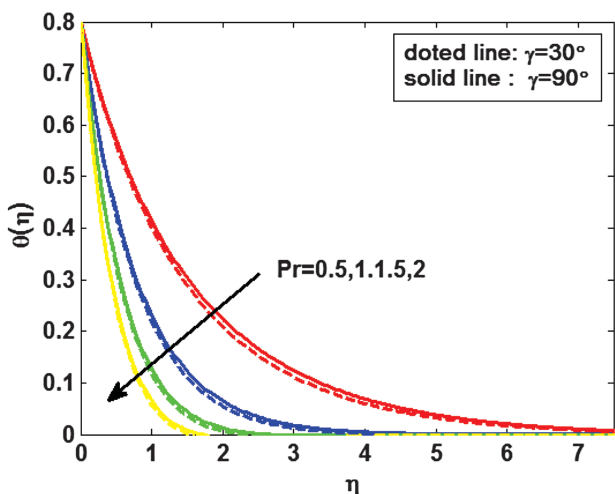


Fig. 5. Effect of prandtl number Pr on temperature profile where $M = 2$, $S = 1$, $\beta = 2$, $R_d = 0.5$, $St = 0.2$.

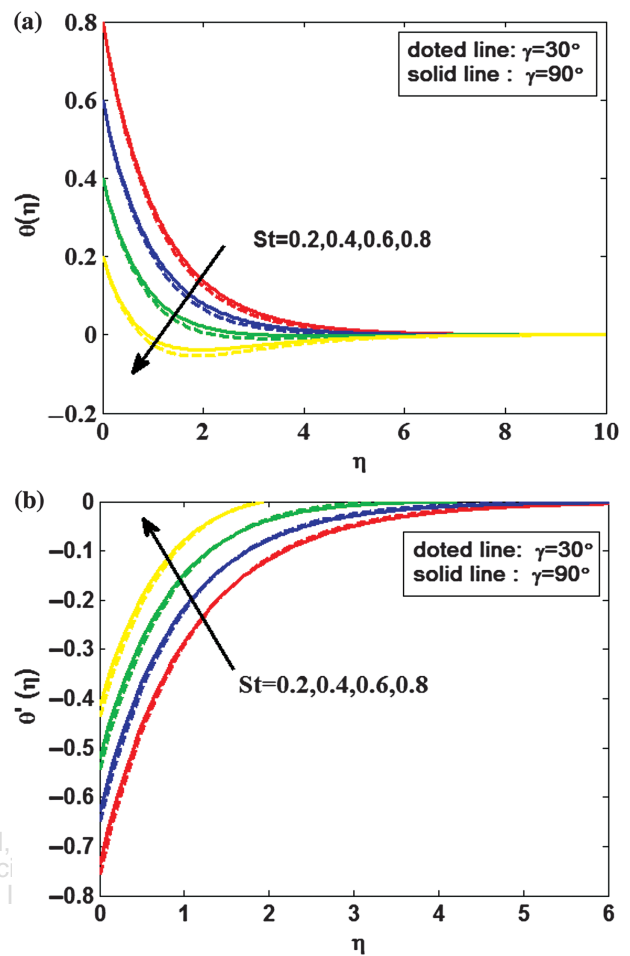


Fig. 6. (a) Effect of stratification parameter St on temperature profile where $Pr = 0.7$, $M = 2$, $S = 1$, $\beta = 2$, $R_d = 0.5$. (b) Effect of stratification parameter St on temperature gradient where $Pr = 0.7$, $M = 2$, $S = 1$, $\beta = 2$, $R_d = 0.5$.

Figures 7(a)–(c) depicts that the variation in velocity profile, temperature profile and temperature gradient for a Casson parameter β respectively. Figure 7(a) shows that the momentum boundary layer thickness is decreasing as an increase in Casson parameter β . The velocity distribution of the fluid is reduced inside the boundary layer away from the surface, but the reverse is true along the surface, the yield stress is decreasing with an increase in Casson parameter. Due to this the resistance force occurred and it makes the fluid velocity decreases. Figure 7(b) represents the variation in temperature profile for various values of Casson parameter β . From the figure the thermal boundary layer thickness is an increase with an increasing the Casson parameter. Figure 7(c) displays the effect of Casson parameter β on the temperature gradient for both the values of aligned magnetic parameter $\gamma = 30^\circ, 90^\circ$. We observe that the temperature gradient increases initially with increasing the Casson parameter β , but finally temperature gradient decreases significantly after a certain distance from the sheet.

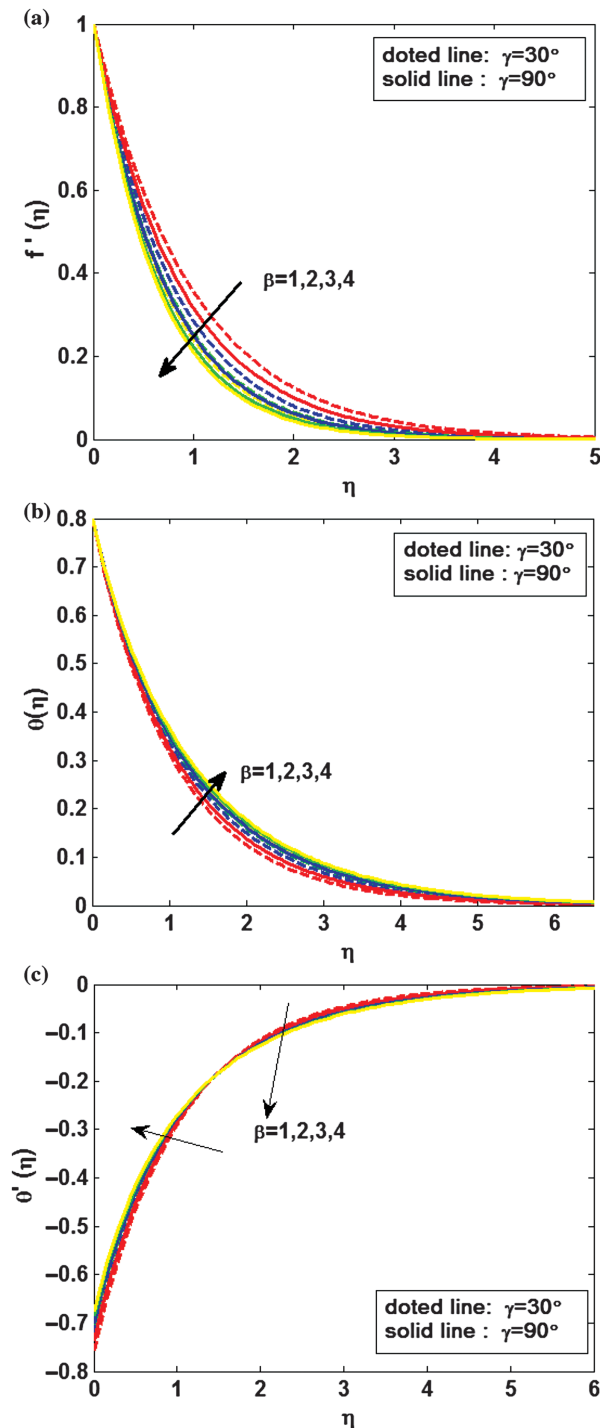


Fig. 7. (a) Effect of casson parameter β on velocity profile where $Pr = 0.7$, $S = 1$, $M = 2$, $R_d = 0.5$, $St = 0.2$. (b) Effect of casson parameter β on temperature profile where $Pr = 0.7$, $M = 2$, $R_d = 0.5$, $S = 1$, $St = 0.2$. (c) Effect of casson parameter β on temperature gradient where $Pr = 0.7$, $M = 2$, $R_d = 0.5$, $S = 1$, $St = 0.2$.

5. CONCLUSION

The Investigation has been carried out numerically to study the effects of Aligned magnetic field and thermal radiation of a Casson fluid over a stretching sheet in

a thermally stratified medium. The transformed nonlinear ordinary differential equations are solved by using the Keller Box Method. The obtained numerical results are compared with previously published work and they are found to be in excellent agreement. The effects of governing parameters on the flow and heat transfer characteristics are thickness presented graphically and quantitatively. The main observations of the present study are as follows:

1. The velocity of the fluid decreases with an increase in Magnetic parameter.
2. The velocity and temperature of the fluid is decrease as an increase in suction parameter where as temperature gradient is increasing.
3. The increasing effect of the radiation parameter increases the temperature distribution.
4. An increment in the Prandtl number decreases the temperature.
5. The temperature profile decreases with an increase in stratification parameter where as temperature gradient increases.
6. The momentum boundary layer thickness decreases with the increase in β . The thermal boundary layer thickness is increasing with the increase in β .

References and Notes

1. K. B. Pavlov, *Magneto hydrodynamics* 10, 146 (1974).
2. Krishendu Bhattacharya, *Journal of Thermodynamics* 2013, Article ID 169674 (2013).
3. Wubshet Ibrahim and Shankar Bandari, *Computers and Fluids* 75, 1 (2013).
4. T. Vijayalaxmi and Shankar Bandari, *J. Nanofluids* 5, 1 (2016).
5. C. Sulochana, N. Sandeep, V. Sugunamma, and B. Rushi Kumar, *Appl. Nanosci.* 6, 737 (2016).
6. J. V. Ramana Reddy, V. Sugunamma, and N. Sandeep, *J. Adv. Phys.* 5, 295 (2016).
7. Prabhakar Bestapu, Shankar Bandari, and Kishore Kumar, *J. Nanofluids* 5, 1 (2016).
8. T. Vijayalaxmi and Shankar Bandary, *J. Nanofluids* 5, 826 (2016).
9. Swati Mukhopadhyay, *Alexandria Engineering Journal* 52, 259 (2013).
10. Tasawar Hayat, Muhammad Farooq, and A. Alsaedi, *International Journal of Numerical Methods for Heat and Fluid Flow* 25, 724 (2015).
11. R. Kandasamy, R. Dharmalingam, and K. K. Sivagnana Prabhu, *Alexandria Eng. J.* 22 (2017), <http://dx.doi.org/10.1016/j.aej.2016.02.029>.
12. P. K. Sarma, T. Subrahmanyam, and V. Dharma Rao, *The Canadian Journal of Chemical Engineering* 68, 38 (1990).
13. Khalil-Ur-Rehman, M. Y. Malik, S. Bilal, and M. Bibi, *Results in Physics* 7, 482 (2017).
14. D. Srinivasacharya and M. Upendar, *J. Egypt. Math. Soc.* 21, 370 (2013).
15. R. Kalaiivanan, P. Renuka, N. Vishnu Ganesh, A. K. Abdul Hakeem, B. Ganga, and S. Saranya, *Procedia Engineering* 127, 531 (2015).
16. B. Prabhakar, Shankar Bandari, and Kishore Kumar, *J. Nanofluids* 5, 1 (2016).
17. S. Mukhopadhyay, *Chin. Phys. B.* 22, 1 (2013).

18. T. Hayat, S. A. Shehzadi, and A. Alsaedi, *Appl. Math. Mech. Engl. Ed.* 33, 1301 (2012).
19. L. J. Crane, *Z Angew Math. Phys.* 21, 645 (1970).
20. M. Subhas Abel, N. Mahesha, and Jagadish Tawade, *Applied Mathematical Modelling* 33, 3430 (2009).
21. M. Wahiduzzaman, Md. Shakhaoath Khan, P. Biswas, Ifsana Karim, and M. S. Uddin, *Applied Mathematics* 6, 547 (2015).
22. P. S. Gupta and A. S. Gupta, *Can. J. Chem. Eng.* 55, 744 (1977).
23. S. Mukhopadhyay, G. C. Layek, and S. A. Samad, *International Journal of Heat and Mass Transfer* 48, 4460 (2005).
24. W. A. Khan and I. Pop, *International Journal of Heat and Mass Transfer* 53, 2477 (2010).
25. Prabhakar Besthapu, Rizwan Ul Haq, Shankar Bandari, and Qasem M. Al-Mdallal, *Neural. Comput. and Applic.* 7 (2017), DOI: [10.1007/s00521-017-2992-x](https://doi.org/10.1007/s00521-017-2992-x).
26. R. Bidin and R. Nazar, *European Journal of Scientific Research* 33, 710 (2009).
27. Y. Dharmender Reddy, V. Srinivasarao, and D. Ramya, *Open Journal of Applied and Theoretical Mathematics* 2, 731 (2016).
28. M. Gnaneswara Reddy, P. Padma, B. Shankar, and B. J. Gireesha, *J. Nanofluids* 5, 1 (2016).
29. H. B. Keller, *Numerical Solutions of Partial Differential Equations*, Academic Press, New York (1971), Vol. II, pp. 327–350.
30. N. M. Sarif, M. Z. Salleha, and R. Nazar, *Procedia Engineering* 53, 542 (2013).

IP: 223.237.59.185 On: Wed, 01 Sep 2021 16:01:10
Copyright: American Scientific Publishers
Delivered by Ingenta